

Nature of Nonexponential Loss of Correlation above the Glass Transition Investigated by Multidimensional NMR

K. Schmidt-Rohr and H. W. Spiess

Max-Planck-Institut für Polymerforschung, Postfach 3148, W-6500 Mainz, Germany

(Received 1 April 1991)

A two-dimensional (2D) and a novel "reduced four-dimensional (4D)" exchange NMR experiment are applied to investigate slow dynamics in poly(vinyl acetate) 20 K above its T_g . The 2D ^{13}C NMR spectra indicate a diffusive process with strongly nonexponential loss of correlation. In the "reduced 4D" experiment, the underlying distribution of correlation times is found to be heterogeneous on the time scale of the average correlation time, becoming homogeneous, however, at later times due to fluctuations which are 2 orders of magnitude slower.

PACS numbers: 64.70.Pf, 61.42.+h, 76.60.-k

The glass transition is a phenomenon common to most amorphous systems.^{1,2} It is marked by drastic changes in the mechanical properties of the material, notably the viscosity. These are directly related to dynamic molecular processes with large amplitudes, which have been studied by many techniques.^{1,2} The average relaxation time τ_0 of the slowest process (α relaxation) exhibits a non-Arrhenius temperature dependence that can be fitted well by the Williams-Landel-Ferry (WLF) function.³ However, the time dependence of this motional process cannot be described by a single exponential. This is inferred from the nonexponential correlation functions measured by relaxation techniques,^{1,2} as well as from two-dimensional exchange ^2H NMR which has shown the simultaneous presence of slow and fast reorientational processes in polymers a few degrees above the caloric T_g .⁴ For temperatures below $T_g + 20$ K, where the mean correlation time is longer than T_1 , ^2H spin-lattice relaxation becomes nonexponential, indicating that the system is heterogeneous (ergodic) on that time scale.⁵ The explanation of such observations has been a matter of dispute for a considerable length of time.^{6,7} They have usually been interpreted in terms of (i) a spatially heterogeneous distribution of correlation times⁸ (parallel processes), or (ii) an intrinsically nonexponential loss of correlation in a homogeneous system (a serial process).

In case (i), the material a few degrees above T_g is thought to consist of clusters of molecules with different rates of motion,⁹ which remain virtually unchanged for a time τ_{fl} exceeding the longest correlation time. Such behavior is sometimes termed nonergodic on a time scale less than τ_{fl} , because within this time a given unit does not probe all the regions in configuration space accessible to other units in the ensemble. Concept (ii) is often related to the Kohlrausch-Williams-Watts (KWW) function,¹⁰ a stretched exponential $\exp[-(t/\tau_0)^\beta]$, $0 < \beta \leq 1$, which yields good fits to most relaxation data. It has been suggested that a natural nonexponential dependence upon time may result from the cooperative nature

of the glass transition process.¹¹ Poly(vinyl acetate) {PVAc, $[-\text{CH}_2-\text{CH}(-\text{O}-\text{C}(=\text{O})-\text{CH}_3)-]_n$ } is considered to be a particularly good example for this.¹¹ The glass transition has been related to a transition from ergodic to nonergodic behavior in mode-coupling theories.¹²

The nature of the nonexponential relaxation behavior can be probed directly if the position or *orientation of the same molecule can be measured at three or more subsequent points in time*, between which substantial loss of correlation occurs. It is the purpose of this Letter to describe a multidimensional NMR technique which achieves this goal and to apply it to the study of the molecular motion in PVAc. In fact, it will be shown that the segmental chain motion is sufficiently heterogeneous to allow for a selection of slow units with $\tau > \tau_0$. After waiting for times $t \gg \tau_0$, some of these units are found to have decreased their correlation times τ significantly, indicating that the heterogeneity is not static.

Solid-state NMR methods can yield information on molecular reorientations due to the dependence of NMR frequencies on the orientation of a given molecular unit relative to the externally applied magnetic field \mathbf{B}_0 :

$$\omega_{\text{aniso}}(\theta, \phi) = (\delta/2)[3 \cos^2(\theta) - 1 - \eta \sin^2(\theta) \cos(2\phi)].$$

Here (θ, ϕ) are the polar angles of \mathbf{B}_0 in the principal-axes system of the chemical-shift tensor, whose orientation with respect to the molecular unit is an inherent property of every type of functional group, as are the parameters δ and η . η is small for the ^{13}C anisotropic chemical shift of the carbonyl carbon of PVAc that will serve as the probe for reorientations, so that mainly θ is relevant and will be used to denote the molecular orientation. Nevertheless, in most of the simulations shown below, $\eta = 0.27$ and the corresponding ϕ dependence are taken into account.

Two-dimensional (2D) exchange NMR¹³⁻¹⁵ on polymers^{4,14} and amorphous silicates¹⁶ has elucidated many details of molecular reorientation geometry.¹⁴ It detects reorientations that occur during the mixing time t_m , cf.

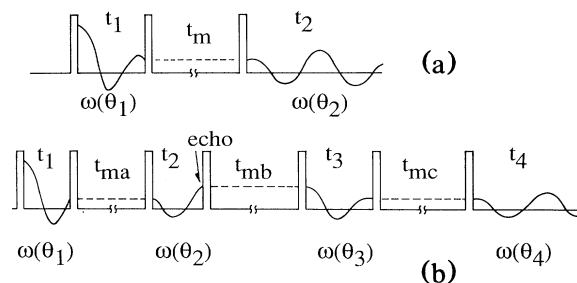


FIG. 1. Schematic pulse sequences for exchange NMR experiments: (a) 2D experiment, (b) 4D experiment. 90° pulses and a typical signal from an isotropic sample are indicated.

Fig. 1(a), by measuring the angular-dependent NMR frequencies before and after t_m . Typically, motions with correlation times in the range $1 \text{ ms} < \tau < 10 \text{ s}$ can be analyzed. The 2D frequency spectrum is generated by two successive Fourier transformations over t_1 and t_2 .^{13,14} It represents the joint probability $S_{2|0}(\omega_1, \omega_2; t_m)$ (Ref. 15) of finding a unit with a frequency ω_1 before t_m , and with frequency ω_2 afterwards, and is plotted in the (ω_1, ω_2) plane. If no reorientation, and consequently no frequency change, takes place during t_m , the spectral intensity is confined to $\omega_1 = \omega_2$, the diagonal of the frequency plane; cf. Fig. 2(a). For reorientations by small angles, the signal appears close to the diagonal. Large angular reorientations give rise to intensity in most parts of the frequency plane.¹⁴ Most important in this study is the simple fact that a ridge along the diagonal of the spectrum reflects the fraction of molecules which have not significantly reoriented during t_m .

Figure 2 shows 2D exchange ^{13}C NMR spectra of the carbonyl carbon (^{13}C in natural abundance) of PVAc taken at a temperature 20 K above its T_g of 300 K. The spectra were acquired with cross polarization and proton decoupling¹⁷ in a ^1H - ^{13}C probe head on a Bruker MSL-300 spectrometer operating at a ^{13}C resonance frequency of 75.47 MHz. With $t_m = 1 \text{ ms}$, a nearly diagonal spectrum is obtained, Fig. 2(a), indicating that little reorientation ("exchange") takes place within this time. On the other hand, the absence of any significant ridge on the diagonal after $t_m = 100 \text{ ms}$, Fig. 2(c), indicates that within this time most molecules have reoriented nearly isotropically. After an intermediate t_m of 10 ms, Fig. 2(b), both the diagonal ridge and large-scale off-diagonal exchange features are simultaneously present. This has been observed likewise in exchange 2D ^2H spectra of polymers above T_g (Ref. 4) and shows that the dynamic process cannot be described by a single correlation time. The spectra can be simulated, however, by accounting for isotropic rotational diffusion with a heterogeneous distribution of correlation times [logarithmic average $\tau_0 = \exp(\ln(\tau))$ of 20 ms, width of approximately 3 decades] as displayed in Fig. 3(a). The curve resembles a KWW distribution function with $\beta = 0.3$.⁶

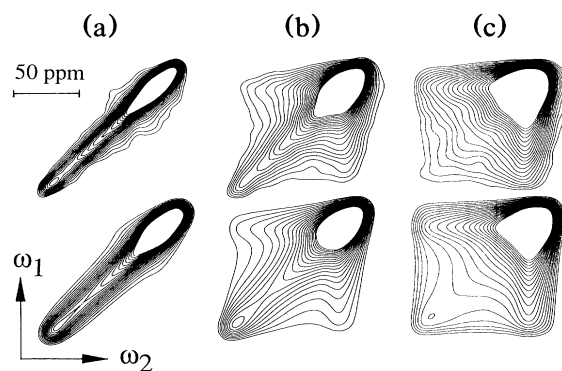


FIG. 2. Upper trace: Contour plots of 2D exchange ^{13}C NMR spectra of PVAc at 320 K for mixing times of (a) 1 ms, (b) 10 ms, and (c) 100 ms. Forty t_1 increments of $24 \mu\text{s}$ were used. Lower trace: Simulated spectra based on rotational diffusion and the distribution of correlation times of Fig. 3(b). The contour lines are linear between 5% and 40% of the maximum, displaying the exchange intensity in detail.

The corresponding correlation function

$$\langle \omega(0)\omega(t_m) \rangle \approx \frac{5}{4} \langle [3 \cos^2\theta(0) - 1][3 \cos^2\theta(t_m) - 1] \rangle$$

is plotted in Fig. 3(b) with data points obtained by appropriate weighted integration of the 2D spectra. As expected, $\langle \omega(0)\omega(t_m) \rangle$ exhibits pronounced nonexponential behavior, even for $t \leq \tau_0$. However, whether the nonexponential loss of correlation is indeed due to a heterogeneous distribution of correlation times cannot be determined using 2D NMR alone.

In order to probe the nature of the distribution a novel "reduced four-dimensional (4D)" exchange experiment has been designed. The magnetization of initially slow units with $\tau_m > \tau_0$ is selected by means of an echo and later characterized in a 2D experiment. From a comparison with the 2D spectrum of all molecules, it can be determined directly whether the units selected in the echo remain slow also at later times. If they do, this proves that the distribution of correlation times is heterogeneous on that longer time scale. The pulse sequence for this experiment, Fig. 1(b), corresponds to that of 4D exchange NMR. It utilizes three mixing times t_{ma} , t_{mb} , and t_{mc} and three evolution periods t_1 , t_2 , and t_3 prior to the signal detection during t_4 . This provides specific information on the molecular orientation at four well-separated points in time. The time signal of 4D exchange NMR is essentially

$$\langle \exp[-i\omega(\theta_1)t_1] \exp[i\omega(\theta_2)t_2] \times \exp[i\omega(\theta_3)t_3] \exp[i\omega(\theta_4)t_4] \rangle,$$

where the brackets indicate the average over all molecules in the sample and θ_1 through θ_4 denote the orientation of the same molecule at four times. A full 4D experiment would require enormous measuring times.

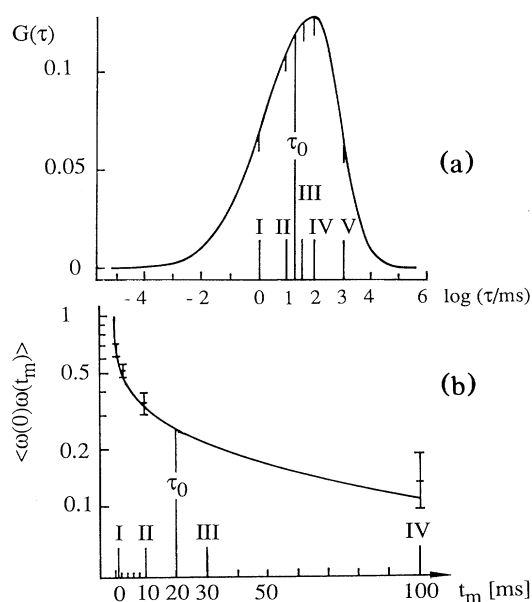


FIG. 3. Plots of (a) the distribution of correlation times as used for the simulations in Fig. 2, and (b) the corresponding correlation function (with experimental data points). I to V refer to the total mixing times used in the experiments.

However, in our reduced version we keep t_1 and t_2 constant and equal. Thus, we work with the magnetization of the stimulated echo that occurs when $t_2 = t_1$. At that point, the magnetization from molecules with $\omega(\theta_1) = \omega(\theta_2)$ adds up coherently, while components which have reoriented substantially during t_{ma} lose correlation between $\omega(\theta_1)$ and $\omega(\theta_2)$, and consequently disappear by destructive interference, provided that t_1 is not too short. Thus, our reduced 4D experiment selects "slow" molecules with $\tau \gg t_{ma}$, and for these it provides the same information as the complete 4D spectrum. A study of the decay of the second stimulated echo generated at $t_4 = t_3$ is not reasonable in PVAc because the signals of the different carbon sites cannot be distinguished in the time domain.

Two reduced 4D spectra are displayed in Fig. 4. The spectrum in Fig. 4(b) was taken with mixing times $t_{ma} = t_{mb} = t_{mc} = 10$ ms, cf. point III in Fig. 3, and effectively represents the 2D spectrum of the slow molecules that give rise to the diagonal contribution in the reference 2D spectrum of Fig. 4(a). In contrast to Fig. 4(a), Fig. 4(b) exhibits intensity almost exclusively on the diagonal. This proves that the selected slow units remain slow on the time scale of $t_{ma} + t_{mb} + t_{mc} \approx \tau_0$. Consequently, the sample cannot be a homogeneous system undergoing a Markov process. In such a system, the echo-selected units, as any subensemble of a homogeneous system, would produce essentially the same 2D spectrum as all units of the system in the nonselective 2D experiment with $t_m = t_{mc}$, in contradiction to the experiments. Thus

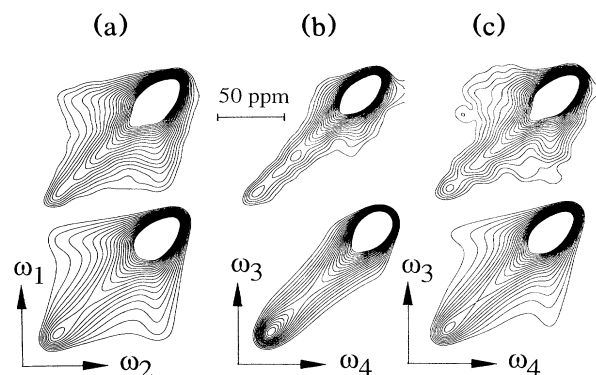


FIG. 4. Exchange ^{13}C NMR spectra of PVAc at 320 K and $t_{ma} = t_{mc} = 10$ ms. (a) Reference 2D spectrum, $t_m = 10$ ms, cf. Fig. 2(b). (b) Reduced 4D spectrum ($t_1 = t_2 = 120 \mu\text{s}$) after a short fluctuation time $t_{mb} = 10$ ms. In the simulation, $\eta = 0$ was assumed for convenience. (c) Reduced 4D spectrum after a long fluctuation time $t_{mb} = 1000$ ms. (b) and (c) correspond to points III and V, respectively, in Fig. 3.

the significantly nonexponential character of the correlation function, cf. Fig. 3(a), is seen to result from a distribution of correlation times that is *heterogeneous on the time scale of τ_0* .

Whether the slow units remain slow on even longer time scales ($t \gg \tau_0$) can also be probed through our reduced 4D experiment by lengthening t_{mb} . In Fig. 4(c) a spectrum for $t_{ma} = t_{mc} = 10$ ms and $t_{mb} = 1000$ ms $= 50\tau_0$ is displayed, cf. point V in Fig. 3. Within 1000 ms the correlation function decays to a value as small as 0.02. The off-diagonal intensity in Fig. 4(c) is markedly higher than in Fig. 4(b). This shows that a significant number of molecules that were initially slow ($\tau > t_{ma} \approx \tau_0$) have *changed their correlation times* to $\tau < \tau_0$ and reorient within $t_{mc} = 10$ ms. Thus in the vitrifying melt, fluctuations are detected that change the reorientational rates of the chain units. This shows that for times $t \gg \tau_0$ the system starts to become *homogeneous (ergodic)*. Still, Fig. 4(c) exhibits less exchange intensity than the reference 2D spectrum Fig. 4(a). Thus, even on a time scale as long as $50\tau_0$ the system shows residual heterogeneity, indicating that significant fluctuations occur only within times on the order of the longest correlation times. Our experiments show that over long times the reorientation of individual segments is *non-Markovian* because their correlation times fluctuate with time.¹⁸ The dynamics of the system as a whole, however, may still exhibit Markovian character.¹⁸

These slow fluctuations, though not producing significant nonexponentiality in the loss of correlation, may be responsible for the asymmetric shape of the distribution of correlation times, a salient feature of Davidson-Cole⁸ and KWW distribution functions.¹¹ In fact, the characteristic times of the fluctuations represent upper limits for all local correlation times, as the large-scale

fluctuations dominate the loss of correlation if the correlation times imposed by the original local environment are too long.

To summarize, our findings can be interpreted within the descriptions of the glass transition mentioned above. For the cluster model they indicate a limited lifetime of the clusters. A similar statement holds for the nonergodic behavior that mode-coupling theory predicts to set in at temperatures well above T_g . Finally, the data show that, in the glass transition, a given molecular unit undergoes non-Markovian motion with time-dependent correlation times, though not on the time scale of the mean correlation time, but rather in a process limiting the longest correlation times.

The reduced 4D experiment is also applicable to nuclei like ^2H , ^{29}Si , and ^{31}P , in a variety of amorphous materials. Variation of the mixing times should yield even more details on the distribution of correlation times. Its temperature dependence may allow one to establish further constraints for theories on the glass transition.

We thank Professor H. Sillescu for helpful discussions, D. Schaefer for assistance with the simulations, and Dr. B. F. Chmelka for carefully checking the manuscript.

¹N. G. McCrum, B. E. Read, and G. Williams, *Anelastic and Dielectric Effects in Polymeric Solids* (Wiley, New York, 1967).

²J. Jäckle, *Rep. Prog. Phys.* **49**, 171 (1986).

³M. L. Williams, R. F. Landel, and J. D. Ferry, *J. Am. Chem. Soc.* **77**, 3701 (1955).

⁴D. Schaefer, H. W. Spiess, U. W. Suter, and W. W. Fleming, *Macromolecules* **23**, 3431 (1990); S. Kaufmann, S.

Wefing, D. Schaefer, and H. W. Spiess, *J. Chem. Phys.* **93**, 197 (1990).

⁵W. Schnauss, F. Fujara, K. Hartmann, and H. Sillescu, *Chem. Phys. Lett.* **166**, 381 (1990).

⁶G. P. Lindsey and G. D. Patterson, *J. Chem. Phys.* **73**, 3348 (1980); P. K. Dixon *et al.*, *Phys. Rev. Lett.* **65**, 1108 (1990).

⁷J. I. Kaplan and A. N. Garroway, *J. Magn. Reson.* **49**, 464 (1982); A. Blumen, I. Klafter, and G. Zumofen, in *Optical Spectroscopy of Glasses*, edited by I. Zschokke (Reidel, Dordrecht, 1986), pp. 199–265.

⁸D. W. Davidson and R. H. Cole, *J. Chem. Phys.* **19**, 1417 (1951).

⁹M. H. Cohen and G. S. Grest, *Phys. Rev. B* **20**, 1077 (1979); **24**, 4091 (1981).

¹⁰G. Williams and D. C. Watts, *Trans. Faraday Soc.* **66**, 80 (1970).

¹¹G. Williams, M. Cook, and P. J. Hains, *J. Chem. Soc. Faraday Trans. II* **2**, 1045 (1972).

¹²U. Bengtzelius, W. Goetze, and A. J. Sjoelander, *J. Phys. C* **17**, 5915 (1984); E. Leutheusser, *Phys. Rev. A* **29**, 2765 (1984).

¹³J. Jeener, B. H. Meier, P. Bachmann, and R. R. Ernst, *J. Chem. Phys.* **71**, 4546 (1979); R. R. Ernst, G. Bodenhausen, and A. Wokaun, *Principles of Nuclear Magnetic Resonance in One and Two Dimensions* (Clarendon, Oxford, 1987).

¹⁴C. Schmidt, B. Blümich, and H. W. Spiess, *J. Magn. Reson.* **79**, 269 (1988); A. Hagemeyer, K. Schmidt-Rohr, and H. W. Spiess, *Adv. Magn. Reson.* **13**, 85 (1989).

¹⁵S. Wefing and H. W. Spiess, *J. Chem. Phys.* **89**, 1219 (1988).

¹⁶I. Farnan and J. F. Stebbins, *J. Non-Cryst. Solids* **124**, 207 (1990).

¹⁷A. Pines, M. G. Gibby, and J. S. Waugh, *J. Chem. Phys.* **59**, 569 (1973).

¹⁸H. Sillescu, *J. Chem. Phys.* **54**, 2110 (1971).